Theoretical Chemistry Accounts (2023) 142:19
https://doi.org/10.1007/s00214-023-02958-1

RESEARCH

$(ZnO)_{42}$ nanocluster: a novel visibly active magic quantum dot under first principle investigation

Bijal R. Mehta[1] · Esha V. Shah[1] · Sutapa Mondal Roy[2] · Debesh R. Roy[1]

Received: 8 September 2022 / Accepted: 13 January 2023 / Published online: 2 February 2023

Abstract

A systematic density functional investigation on the structural, electronic and optical properties of the growth of $(ZnO)_6$ cluster unit in the series of $(ZnO)_{6n}$ for $n = 1$–9 is reported in this paper. Different electronic properties of $(ZnO)_{6n}$ nanoclusters are analyzed in terms of HOMO–LUMO gap (HLG), ionization potential (IP), electron affinity (EA), chemical hardness (η) and electrophilicity index (ω), which all shows a zigzag behavior as the size of $(ZnO)_{6n}$ clusters increases. The electronic energy gain (ΔE) of the clusters identified an exceptionally stable 'magic' nanocluster, viz. $(ZnO)_{42}$. Frontier orbitals analysis results indicate easy electron transfer in $(ZnO)_{42}$ nanocluster system. The optical absorption spectra confirm that the magic $(ZnO)_{42}$ nanocluster is active in the visible range ($\lambda = 406.8$ Å) of electromagnetic spectrum. Interestingly, like zigzag electronic properties, similar optical switching toward the growth of $(ZnO)_6$ unit is also observed. The simulation results of electronic properties as well as the infrared spectra of magic $(ZnO)_{42}$ cluster will open up a vista to the experimentalists for its possible synthesis, which in turn will help in the development of the visibly active magic $(ZnO)_{42}$ nanocluster with novel applications in the fields of quantum dots or assembled materials.

Keywords Zinc oxide nanoclusters · Magic cluster · Quantum dot · Infrared spectra · Density functional theory

1 Introduction

Fine particles having diameters of a few angstroms to a few nanometers often tend to change their properties with the addition of even a single atom due to their high surface density. These fine particles are well-known as atomic clusters [1]. Such clusters mainly consist of fewer to thousands of atoms constituting an intermediate state of matter in atoms, molecules, and solids. In any cluster, its size and composition can be controlled by a single atom at a time that helps to interpret how the properties of bulk matter evolve. Therefore, the clusters are of significant research interest as they possess unique properties, which are sometimes quite different from their bulk counterpart [1–11]. For instance, small clusters of Mn are ferromagnetic, whereas Mn is antiferromagnetic in its bulk form [12, 13]. In addition, they exhibit unique physical and chemical properties and are likely to show large applications in many fields, such as optical, magnetism, catalytic, and nanoelectronics. These specific properties are due to various factors, including the very high ratio of surface-to-volume, related to the Jellium model of electronic shell closings, geometrical high symmetry, super atomic behavior and quantum confinement [1–11].

Due to these characteristics, the materials appear essential for heterogeneous catalysis, where the selectivity and activity of heterogeneous catalytic reactions can probably be modified through minor changes in the cluster size and composition.

Metal oxides are of great technological interest due to their applications in various fields such as heterogeneous catalysis in chemical processes that produce fuel and

Bijal R. Mehta and Esha V. Shah. Shah have contributed equally to this work.

The authors dedicate this work to Professor Pratim Kumar Chattaraj on his 65th birth anniversary.

✉ Sutapa Mondal Roy
smr@ptscience.ac.in

✉ Debesh R. Roy
drr@phy.svnit.ac.in

[1] Materials and Biophysics Group, Department of Physics, Sardar Vallabhbhai National Institute of Technology, Surat 395007, India

[2] Sir P. T. Sarvajanik College of Science, Veer Narmad South Gujarat University, Surat 395001, India

value-added chemicals as well as in microelectronics, where surface stability is a valuable characteristic of material [14, 15]. In addition, metal oxides are well-known for their industrial applications, such as surface catalytic properties as oxidation catalysts and adsorbents for toxic chemical agents [16].

Zinc oxide (ZnO) is considered to be an intriguing material toward the evolution of exciton-based optoelectronic devices such as light-emitting diode (LEDs) and photovoltaic cells having a direct bandgap of 3.3 eV at room temperature [17]. Furthermore, a large exciton binding energy of 60 meV can exceed even above room temperature based on exciton recombination for lasing action [18, 19]. In addition, ZnO is a potential material for space applications due to its tendency to remain stable in high-energy radiation environment and its affability toward wet chemical etching. Further, ZnO etches with ease compared to many other acids and alkalis can be fabricated by a pure crystal growth method, thereby assisting in developing low-cost and small-size ZnO-based devices. In addition, ZnO is non-toxic, sustainable and cost-effective**.** These characteristics of ZnO make it suitable for diverse applications in various fields including photonics, electronics, sensing and energy harvesting [20]. Recently, one- dimensional ZnO nanowires (NWs) have gained much interest due to their recognition in gas sensors and ultraviolet (UV) optoelectronic devices like photodetectors [21], dye-sensitized solar cells [22, 23] light-emitting diodes [24] and biomedical applications [25]. Although, zinc oxide displays momentous performance as bulk (3D), nanowires (1D) and nanosheets (2D), but discovery of its novel and potential quantum dots (0D) especially through the investigation on their nanoclusters with exceptional physicochemical properties remain a challenging task.

It is observed in past that certain atomic clusters comprising of specific number of atoms of an element or alloy, show exceptional stability compared to their neighboring atomic clusters in a considered series of a cluster unit. Such atomic clusters are known as 'magic clusters', and the number of atoms composing the magic cluster is called the 'magic number' [26]. The "magic number" is an elemental property of atomic clusters and therefore usually differs depending on respective constituent elements. For example, the magic number of neutral gold atomic clusters is 55 [27], and that of neutral silver atomic clusters is 20 [28]. In experiments, magic clusters in a series of atomic clusters of an element (or a compound) are identified through mass spectroscopy. The spectrum shows prominent and distinguished ultra-high peaks for the magic clusters in the considered series. The studies by Kukreja et al. [29] and Dmytruk et al. [30] on the experimental synthesis of zinc oxide ionic clusters by laser ablation and mass spectrometry techniques report magic numbers of $n = 34$, 60 and 78 for zinc oxide atomic clusters series $(ZnO)_n$. A theoretical study by Chen et al. [31] identifies $n = 78$, 100, 132 and 168 for $(ZnO)_n$ atomic cluster series as magic numbers. It is interesting to note from the literature that in most of the cases, ZnO clusters in the form of $(ZnO)_n$, acquires magic stability when values of n are in multiples of six [32]. This understanding has motivated us to look for novel magic nanoclusters (quantum dot) with promising application in the series of $(ZnO)_{6n}$ clusters.

The present study aims in-depth scrutiny of structure and physicochemical properties of $(ZnO)_{6n}$ atomic clusters for $n = 1$–9. The minimized geometries, electronic and optical properties of the atomic clusters are evaluated under density functional theory [33–35]. The quantum chemical parameters, namely HOMO–LUMO gap (HLG), ionization potential (IP), electron affinity (EA), chemical hardness (η), electrophility index (ω), total energy gain (ΔE) accounts for the stability, energetic and electronic properties of the considered $(ZnO)_n$ clusters. The analysis of energy gain (ΔE) identifies $(ZnO)_{42}$ as exceptionally stable magic cluster in the series. Further, to understand the precise cause of reactivity and stability of the clusters the Frontier Molecular Orbital's (FMOs) are analyzed. In order to identify the optical activity of the $(ZnO)_{6n}$ ($n = 1$–9) clusters series in the electromagnetic spectrum, their UV–Vis absorption spectra are calculated and compared. The UV–Vis spectra reveal that the magic $(ZnO)_{42}$ nanocluster is a visibly active quantum dot with multi-fold future promises. Finally, in order to guide experimentalists for the possible synthesis of optically active magic $(ZnO)_{42}$ nanocluster, we have reported critical analysis of its infrared (IR) spectra and important vibrational modes.

2 Theory and computation

The geometry optimization and various physicochemical properties of $(ZnO)_{6n}$ ($n = 1$–9) nanoclusters were carried out under the framework of density functional theory (DFT) [33–35]. A molecular orbital method is adapted using a linear combination of atomic orbitals (LCAO) to examine the electronic structure. In order to predict the global minimum structures, a large pool of isomers is considered as initial structures which also include the reported structures by Chen et al. [31], in which they performed global geometry optimization of $(ZnO)_n$ for $n \leq 168$ using an evolutionary hybrid genetic algorithm (HGA) with the energetics obtained using semi-empirical molecular orbital theory with the MNDO/MNDO/d. Moreover, they have confirmed the global minima through optimizing all those HGA obtained structures by standard DFT level of B3LYP|DZVP2. In the present study, in order to reconfirm the global minima of these clusters, we have added many more hand/machine modeled isomers (cage like/unlike) in our study. For the stability prediction of hybrid molecular structures, Becke 3-parameter exchange

and Lee–Yang–Parr correlation (B3LYP) functional, as introduced by A. D. Becke [36], is employed in the Hamiltonian. The standard Los Alamos ECP plus D.Z. (LANL2DZ) used extensively as the basis set in this work, which includes scalar relativistic correction [37, 38]. For optimizing the considered clusters, the convergence tolerance (threshold) for maximum force is considered to be 1.5×10^{-5} Hartree/Bohr, whereas tolerance limit for displacement is considered to be 6.0×10^{-5} Angstrom. In order to check any effect of basis set, we also have used another popular and reliable basis set LANL2MB which uses Los Alamos ECP plus MBS [39], and compared with LANL2DZ basis set. The actual calculations were carried out using suits of codes as implemented in GAUSSIAN 09 program [40]. Various electronic properties, namely, energy gap (HLG) between the highest occupied (ϵ_{HOMO}) and lowest unoccupied (ϵ_{LUMO}) molecular orbitals, ionization potential (IP), electron affinity (EA), chemical hardness (η) and electrophilicity index (ω) were calculated using conceptual density functional theory (CDFT) [35, 41].

The electronic parameters were calculated using the standard formulations as prescribed by the conceptual density functional theory (CDFT) [35, 41]. The energy gap (HLG) between the highest occupied (ϵ_{HOMO}) and lowest unoccupied (ϵ_{LUMO}) molecular orbitals energies is calculated as follows:

$$\mathrm{HLG} = \epsilon_{\mathrm{LUMO}} - \epsilon_{\mathrm{HOMO}} \tag{1}$$

The ionization potential (IP) and electron affinity (EA) were calculated using the Koopmans' theorem as follows [35, 41],

$$\mathrm{IP} \approx -\epsilon_{\mathrm{HOMO}};\ \mathrm{EA} \approx -\epsilon_{\mathrm{LUMO}} \tag{2}$$

Chemical potential (μ) [35, 41] is defined as the first derivative of total electronic energy (E) in respect to the total number of electrons (N), at a constant external potential v(r):

$$\mu = \left[\frac{\partial E}{\partial N}\right]_{v(\vec{r})} \tag{3}$$

Using a finite difference approach, μ may be presented in terms of ionization potential (IP) and electron affinity (EA) as follows:

$$\mu = -\frac{\mathrm{IP} + \mathrm{EA}}{2} \tag{4}$$

The electronegativity (χ) can be defined as the negative of chemical potential (μ) as follows [35, 41]:

$$\chi = -\mu = -\left[\frac{\partial E}{\partial N}\right]_{v(\vec{r})} \tag{5}$$

R. G. Pearson [42, 43] has reported that chemical hardness (η) correlates in general with stability and reactivity for a chemical structure. The η usually resists electron distribution or transferring of a charge in a molecule. The chemical hardness is defined as follow:

$$\eta = \frac{1}{2}\left(\frac{\partial^2 E}{\partial N^2}\right)_{v(\vec{r})} \tag{6}$$

where E is the total electronic energy, N is the total number of electrons, at a constant external potential $v(r)$. Using finite difference methods, and η can be expressed in terms of ϵ_{HOMO} and ϵ_{LUMO} as follows:

$$\eta = \left(\epsilon_{\mathrm{LUMO}} - \epsilon_{\mathrm{HOMO}}\right)/2 \tag{7}$$

The electrophilicity index (ω) is define as follows [44–46]:

$$\omega = \mu^2/2\eta \tag{8}$$

The electrophilicity index measures the propensity or the capacity of a species to accept electrons. The ω is the measure of the stabilization in energy after a system accepts the additional amount of electronic charge from the environment.

The energy gain (ΔE) of a $(\mathrm{ZnO})_{6n}$ nanocluster in assembling a $(\mathrm{ZnO})_6$ unit to its previous cluster $(\mathrm{ZnO})_{6(n-1)}$ is calculated as follows:

$$\Delta E = E\left[(\mathrm{ZnO})_6\right] + E\left[(\mathrm{ZnO})_{6(n-1)}\right] - E\left[(\mathrm{ZnO})_{6n}\right] \tag{9}$$

where E $[(\mathrm{ZnO})_6]$, E $[(\mathrm{ZnO})_{6(n-1)}]$ and E $[(\mathrm{ZnO})_{6n}]$ are the total energies of the $(\mathrm{ZnO})_{6(n-1)}$ and $(\mathrm{ZnO})_{6n}$ nanoclusters, respectively.

To obtain optical absorption spectra (UV–Vis), we have carried out excited state calculations for all the considered compounds under time-dependent density functional theory (TDDFT) formalism, which may be understood as an exact reformulation of time-dependent quantum mechanics where particle states are replaced by density of states [47, 48]. Through such approach, a set of modified Kohn–Sham equations describe the evolution of electron density using non-interacting electrons in an effective exchange–correlation time-dependent functional. Excitation energies are obtained by analyzing the response of the considered system to small time-dependent perturbations. The actual calculations are performed utilizing GAUSSIAN 09 [40] code where thirty lowest singlet–singlet vertical electronic excitations were requested keeping the same functional and basis set. On the other hand, it is known that for a vibrating molecule, infrared bands arise due to the interaction between light and oscillating dipole moment [49]. For computation of IR spectra, harmonic vibrational frequencies and infrared intensities were calculated using the analytical second derivatives for ab initio methods and numerical differentiation of analytical gradients in the considered DFT method. To obtain the

normal modes in a molecule-fixed coordinate system, the non-redundant set of internal coordinates was considered as proposed by Fogarasi and Pulay [49]. The calculated potential energy distribution (PED) matrices [50] enable to obtain detailed information of the vibrational bands. The transmittance (%T) is calculated from the simulated molar absorptivity (ε) using Beer–Lambert law [51, 52].

3 Results and discussion

Figure 1 represents below shows the optimized structures for the zinc oxide nanoclusters, namely, $(ZnO)_{6n}$ ($n=1$–9). The representative geometrical parameters of $(ZnO)_{6n}$ clusters are also provided. It is intriguing to perceive that all the considered clusters exhibit good symmetries except for $(ZnO)_{54}$ (C_1) as reported in Table 1. It may be noted that geometries of all the optimized nine $(ZnO)_{6n}$ nanoclusters in the present work at B3LYP|LANL2DZ level of theory looks similar to those reported by Chen et al. [27] in past at a lower level of semi-empirical MNDO/MNDO/d calculations through genetic algorithm approach.

Successful convergence of forces and atomic displacements gives minimized energy bond length between zinc and oxygen atoms as 1.95 Å as observed in $(ZnO)_6$. The $(ZnO)_6$ shows two hexagonal rings on top to bottom with alternative arrangement of Zn and O atoms with D_{3d} symmetry. The following $(ZnO)_{6n}$ nanoclusters with $n=2$, 3 and

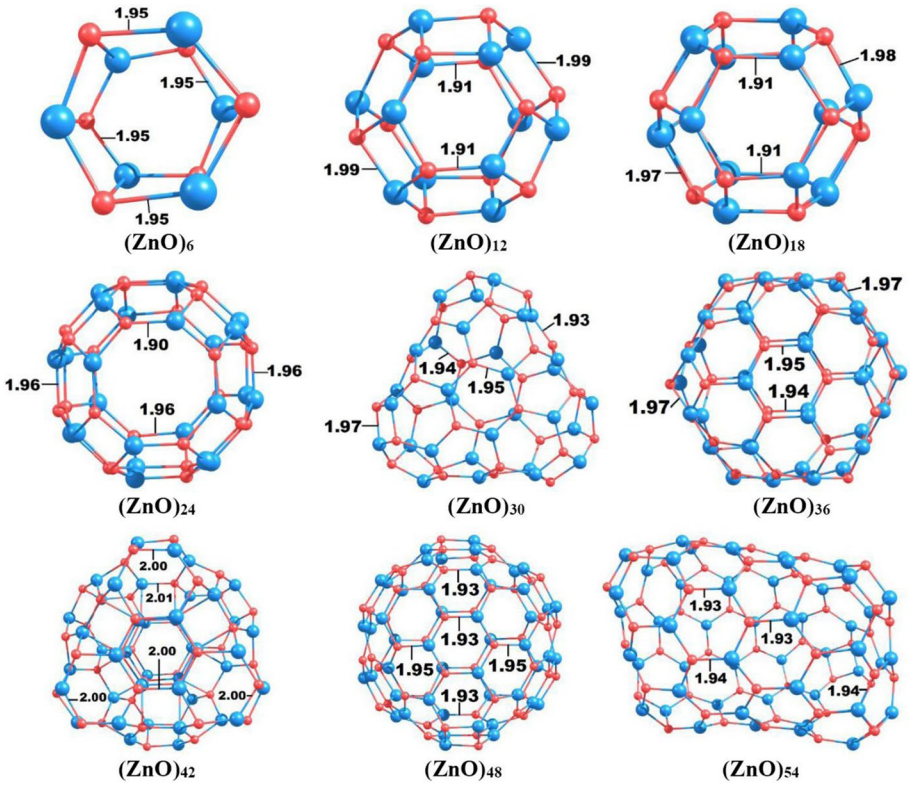

Fig. 1 Optimized geometries of the zinc oxide nanoclusters: $(ZnO)_{6n}$ ($n=1$–9)

Table 1 Point group symmetry (PG), HOMO–LUMO gap (HLG), ionization potential (IP), electron affinity (EA), chemical hardness (η) and electrophilicity index (ω) of the $(ZnO)_{6n}$ ($n=1$–9) nanoclusters at B3LYP functional with LANL2DZ (B1) and LANL2MB (B2) basis sets level of calculations

n	PG	HLG		IP		EA		η		ω	
		B1	B2	B1	B2	B1	B2	B1	B2	B1	B2
1	$^{D}3d$	3.47	1.81	6.52	5.54	3.06	3.73	1.73	0.90	6.63	11.87
2	S_6	4.04	2.30	6.83	5.88	2.80	3.57	2.02	1.15	5.74	9.68
3	S_6	3.87	2.17	6.71	5.78	2.84	3.61	1.94	1.09	5.88	10.14
4	S_8	3.99	2.32	6.72	5.77	2.73	3.45	1.99	1.16	5.59	9.16
5	C_3	3.74	2.16	6.62	5.79	2.88	3.63	1.87	1.08	6.03	10.26
6	T_d	3.82	2.22	6.67	5.79	2.84	3.57	1.91	1.11	5.91	9.87
7	S_6	3.49	1.78	6.57	5.63	3.08	3.85	1.74	0.89	6.68	12.62
8	S_6	3.89	2.31	6.64	5.82	2.75	3.50	1.95	1.16	5.67	9.40
9	C_1	3.86	2.23	6.61	5.74	2.76	3.51	1.93	1.11	5.69	9.59

4 shows fullerene-like structures with S_6, S_6 and S_8 symmetries. The minimized structure of $(ZnO)_{30}$ cluster appears to be a closed triangular fullerene-like structure with C_3 symmetry, whereas $(ZnO)_{36}$ is found with T_d symmetry. The lowest energy configurations of $(ZnO)_{42}$ and $(ZnO)_{48}$ were found with S_6 symmetry with combination of hexagonal and tetragonally architected rings. The $(ZnO)_{54}$ cluster is found to be the least symmetric (C_1) in the series. The range of optimized bond lengths in the considered $(ZnO)_{6n}$ ($n = 1$–9) is found to be from 1.90 to 2.01 Å.

In order to understand structural and electronic properties, and reactivity of the considered series of $(ZnO)_{6n}$ nanoclusters, various descriptors in light of conceptual density functional theory [31, 37] has been calculated. The point group symmetry (PG), HOMO–LUMO energy gap (HLG), ionization potential (IP), electron Affinity (EA), chemical hardness (η) and electrophilicity index (ω) are provided in Table 1.

It may be noted from Table 1 that larger IP (> 6 eV) and η (~ 2 eV) for all the $(ZnO)_{6n}$ nanoclusters indicate their stability in general, whereas large EA (~ 3 eV) indicates their higher affinity for assembling with the similar cluster units. It is very interesting to note that a zigzag behavior is observed in all the electronic descriptors (HLG, IP, EA, η and ω) along the growth of $(ZnO)_6$ unit in the $(ZnO)_{6n}$ series, as reported in Table 1. A better visualization of this observation is presented in Fig. 2. In order to recheck such zigzag behavior and the electronic properties, we have also studied the effect of another popular basis set LANL2MB as provided in Table 1. It may be noted that the additional basis set shows the similar zigzag behavior in the electronic properties of $(ZnO)_{6n}$ series along the growth of $(ZnO)_6$ unit. The tunability of electronic properties in every sixth zinc oxide cluster unit may possibly be a useful information to control physicochemical properties of ZnO nanoclusters/quantum dots during their growth. It may be noted from Fig. 2 that the 'even n (= 2, 4, 6, 8)' in $(ZnO)_{6n}$ series correspond to the higher values of the stability related electronic properties, viz. homo–lumo gap (HLG), ionization potential (IP) and chemical hardness (η), compared to their 'odd n (= 1, 3, 5, 7, 9)' neighbors. On the other hand, 'odd n' values correspond to the higher values of reactivity related properties like electron affinity (EA) and electrophilicity (ω), compared to their 'even n' neighbors, as expected. Such correspondence of 'even/odd n' zigzag pattern to the stability/reactivity related electronic properties may be understood as higher stability of the $(ZnO)_{6n}$ clusters for 'even n' in general; however, it needs a careful scrutiny.

Figure 3 represents the energy gain (ΔE) of $(ZnO)_{6n}$; $n = 2$–9 nanoclusters for adding one $(ZnO)_6$ unit to their previous size. It is interesting to note that $(ZnO)_{42}$ revealed to be an exceptionally stable 'magic' nanocluster with highest energy gain (1.26 eV) in the series. It also interestingly be noted from Fig. 2 that whereas the lower HLG (3.49 eV), ionization potential (6.57 eV) and chemical hardness (1.74 eV) of $(ZnO)_{42}$ in the series indicates easy electron transmission in the system, its highest electron affinity (3.08 eV) and electrophilicity (6.68 eV) implies its excellent tendency to assemble with similar cluster units toward forming novel cluster assembled material for diverse applications. Overall, magic stability and highest affinity of $(ZnO)_{42}$ nanocluster reveal this cluster as a novel unit for quantum dot and cluster assembled materials with useful applications.

In order to gain more insight into the orbital electronic distribution and absorption domain of $(ZnO)_{42}$ magic cluster in the electromagnetic spectra, we have carried out its frontier molecular orbital (FMO) analysis and optical absorption spectra (OAS).

Frontier molecular orbitals (FMO) play a vital role in chemical selectivity and reactivity. Figure 4 represents few important molecular orbitals of $(ZnO)_{42}$, viz. from HOMO-2

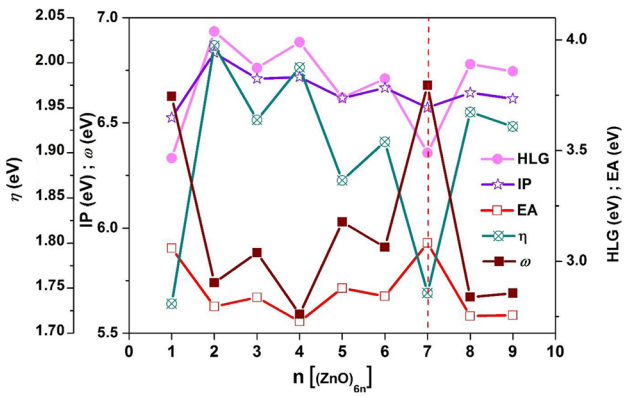

Fig. 2 Electronic properties of the zinc oxide nanoclusters, viz. $(ZnO)_{6n}$ ($n = 1$–9)

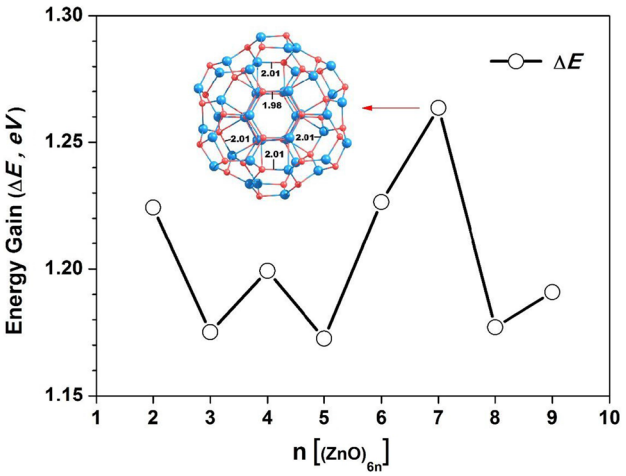

Fig. 3 Energy gain of the zinc oxide nanoclusters, viz. $(ZnO)_{6n}$ ($n = 2$–9)

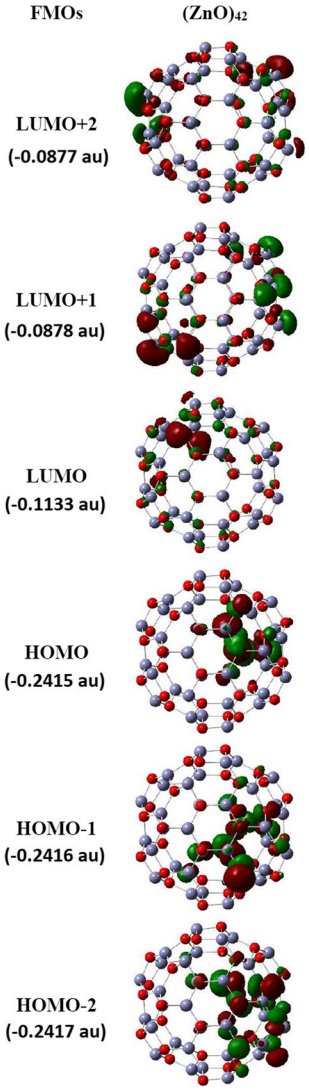

Fig. 4 Frontier molecular orbitals (FMOs) of $(ZnO)_{42}$ magic nanocluster. The energies of the various FMOs are also mentioned in atomic unit (au)

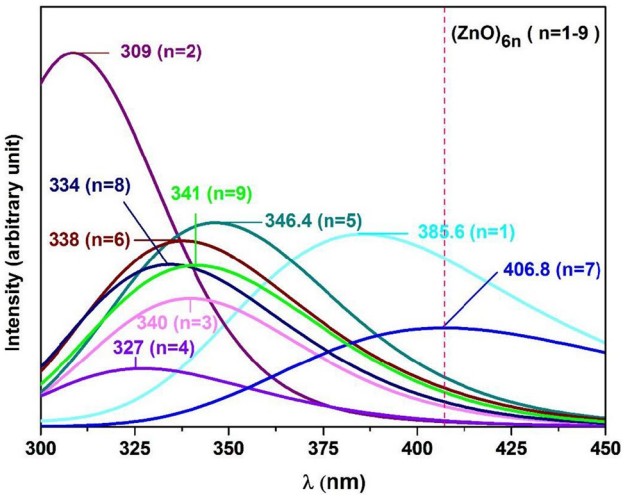

Fig. 5 Optical absorption spectra of zinc oxide nanoclusters, viz. $(ZnO)_{6n}$ ($n = 1$–9)

until LUMO + 2, whereas the respective orbitals are presented by fixing the position of the cluster. It is very interesting to note that there is no coincidence of the electronic lobes for HOMO and LUMO, implying a strong affinity at the LUMO to attract electron from HOMO which facilitates easy electron transfer. Further, the possible distribution of electron density in the higher virtual orbitals than LUMO, e.g., LUMO + 1 and LUMO + 2 also show additional (or alternate) domains that also support the probable easy electron transfer from HOMO to those virtual orbitals in $(ZnO)_{42}$, as expected from its highest electron affinity in the series (Table 1). In order to understand atomic charge distribution at various atomic centers in $(ZnO)_{42}$ magi nanocluster, we have carried out Mulliken population analysis [53]. The charge distribution on various atoms in the magic $(ZnO)_{42}$ cluster in Table S1 in the Supplementary Information. It is observed that atomic charges are symmetrically distributed in the Zn and O centers, whereas Zn atoms shows electron deficient centers (with positive fractional charges) and O atoms shows electron rich centers (with negative fractional charges). The absolute dipole moment values for $(ZnO)_{6n}$ clusters are also reported in Table S2 in Supplementary Information. A zigzag pattern is noticed with increase in 'n' similar to electronic properties, except for $n = 5$.

Optical absorption spectra (UV–Vis) of $(ZnO)_{6n}$ ($n = 1$–9) nanoclusters are presented in Fig. 5. It is again interesting to note a zigzag pattern in the wavelengths associated to intensity maxima (peak) is observed along the growth direction in the series, as noticed on the electronic properties (Fig. 2). Such optical switching behavior may be a useful information for possible applications of these clusters. It is also very intriguing to observe that although all the zinc oxide clusters are found to be ultraviolet active (wavelength ranging from 309 nm to 385.6 nm), the magic $(ZnO)_{42}$ nanocluster reveal to be a visibly active ($\lambda = 406.8$ nm) nanocluster in the series. Therefore, in addition to the exceptional stability and affinity of $(ZnO)_{42}$ cluster, visibly active nature of this magic nanocluster will certainly find novel semiconductor and optoelectronic future applications in its relevant quantum dots and assembled materials.

In order to understand detailed structural information on $(ZnO)_{42}$ nanocluster, which would help experimentalists for the development of possible synthesis schemes for quantum dot or assembled materials, we have simulated its vibrational analysis in terms of infrared spectra (IR) as presented in Fig. 6. The major harmonic frequencies (ω) and infrared intensities (I) and their respective vibrational assignments are provided in Table 2. The vibrational assignments are

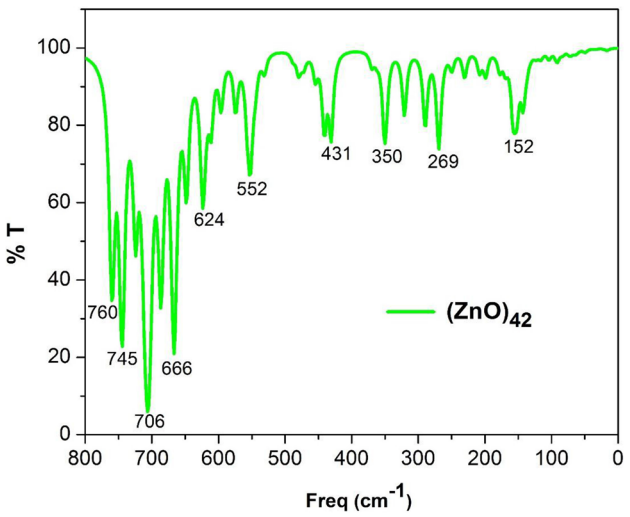

Fig. 6 Infrared spectroscopy (IR) spectra of the magic $(ZnO)_{42}$ quantum dot

Table 2 Major harmonic frequencies (ω, cm^{-1}) and infrared intensities (I, km/mol), and their respective vibrational assignments for $(ZnO)_{42}$ nanocluster

No	ω	I	Assignment†
1	152	76	ν^{as} (O–Zn)
2	269	183	ν^{as} (O–Zn)
3	350	142	ν^{as} (O–Zn)
4	431	214	ν^{s} (O–Zn)
5	552	389	τ (Zn–O)
6	624	229	ν^{as} (O–Zn)
7	666	893	ν^{s} (O–Zn)
8	706	1496	ν^{as} (O–Zn)
9	745	873	ν^{s} (O–Zn)
10	760	1219	ν^{s} (O–Zn)

†ν^{s}: symmetric stretching, ν^{as}: asymmetric stretching, τ: torsion

obtained in terms of symmetric stretching (ν^{s}), asymmetric stretching (ν^{as}) and torsion (τ) modes. In the lower IR, notable modes are found at 152 cm^{-1}, 269 cm^{-1} and 350 cm^{-1} for the asymmetric stretching (ν^{as}) of O–Zn bonds in the cluster. The mid IR vibrations are noticed at 431 cm^{-1} (ν^{s}), 624 cm^{-1} (ν^{as}) and 666 cm^{-1} (ν^{s}) on O–Zn bonds, and 552 cm^{-1} (τ) on Zn–O moieties. The characteristic modes in the higher rang IR spectrum are noticed at 706 cm^{-1} (ν^{as}), 745 cm^{-1} (ν^{s}) and 760 cm^{-1} (ν^{s}) on O–Zn bonds.

The visualization of some most important representative vibrational modes is presented in Fig. 7. The above results on the critically analyzed vibrational spectra of $(ZnO)_{42}$ nanocluster will certainly help experimentalists for possible synthesis of this novel visibly active magic nanocluster for its possible optoelectronic applications as quantum dots or assembled materials.

4 Conclusions

In summary, systematic and detailed investigation on various electronic properties, viz. HLG, IP, EA, η and ω reveal a zigzag behavioral pattern for the growth of every sixth ZnO units in the series of $(ZnO)_{6n}$; for $n = 1$–9 nanoclusters. The energy gain (ΔE) calculations on $(ZnO)_{6n}$ clusters identified $(ZnO)_{42}$ as an exceptionally stable 'magic' nanocluster in the series. The lower HLG, IP and η values of $(ZnO)_{42}$, facilitates easy electron transfer in the system. The highest EA and ω values of $(ZnO)_{42}$ implies its excellent tendency toward novel assembly with similar cluster units. The frontier molecular orbital analysis also supports easy electron transferal nature in the system. It is intriguing to note that the magic $(ZnO)_{42}$ nanocluster is active in the visible range ($\lambda = 406.8$ Å) of the electromagnetic spectrum. Also, interestingly, similar to the electronic properties, a zigzag optical switching is also observed toward the growth for every sixth ZnO units in the $(ZnO)_{6n}$ cluster series. In order to gain more insight on the possible synthetic routes of optically active and magic $(ZnO)_{42}$ nanocluster, detailed simulated infrared

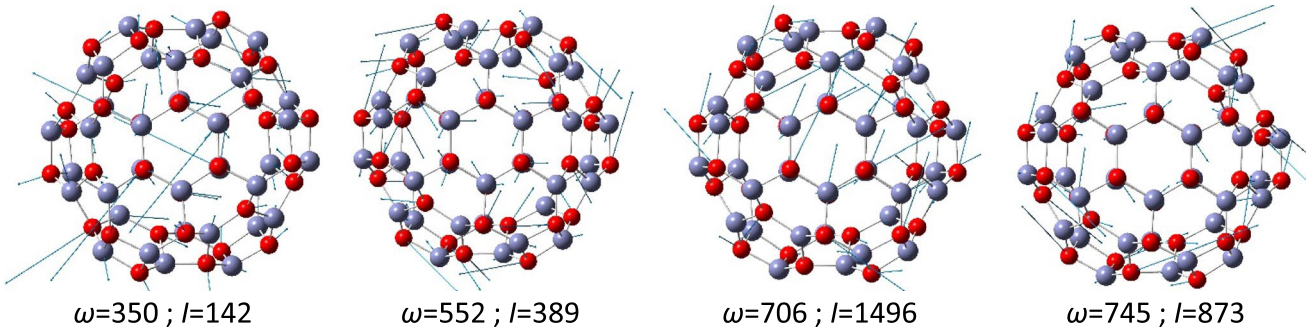

Fig. 7 Some representative major infrared vibrational modes of $(ZnO)_{42}$ nanocluster

spectra and various modes and characteristic frequencies of the cluster have been predicted, which would help the experimentalists. The results in the present work revealed the $(ZnO)_{42}$ as a novel visibly active magic nanocluster, which would find future novel applications in the form of quantum dots or assembled materials in the semiconductor and optoelectronic industries.

Supplementary Information The online version contains supplementary material available at https://doi.org/10.1007/s00214-023-02958-1.

Acknowledgements DRR is thankful to the SERB, New Delhi, Govt. of India for financial support (Grant Nos. EMR/2016/005830 and CRG/2020/002634). SMR is thankful to the SERB, New Delhi, Govt. of India for financial support (Grant No. TAR/2021/000150).

Authors contribution BRM contributed to investigation, results, and writing—original draft. EVS contributed to investigation, results, and writing—original draft. SMR contributed to conceptualization, supervision, results analysis, writing—review and editing. DRR contributed to conceptualization, supervision, results analysis, writingβ—review and editing, resources.

Declarations

Conflicts of interest The authors declare no competing financial interest.

References

1. Jena P, Khanna SN, Rao BK (1999) (1999) Theory of atomic and molecular clusters 27–53. Springer
2. Kappes MM, Kunz RW, Schumacher E (1982) Production of large sodium clusters (Na_x, $x < 65$) by seeded beam expansions. Chem Phys Lett 91:413–418
3. Ekardt W (1984) Dynamical polarizability of small metal particles - self-consistent spherical jellium background model. Phys Rev Lett 52:1925–1928
4. Bergeron DE, Castleman AW, Morisato T, Khanna SN (2004) Formation of $Al_{13}I^-$: evidence for the superhalogen character of Al_{13}^-. Science 304:84–87
5. Knight WD et al (1984) Electronic shell structure and abundances of sodium clusters. Phys Rev Lett 52:2141–2143
6. Roy DR, Singh PK (2013) Magic stability of Ga_4Mg_3 cluster in Ga_xMg_3 (x=1-6) series: a density functional study. Chem Phys 411:6–10
7. Khatua S, Roy DR, Chattaraj PK, Bhattacharjee M (2007) Synthesis and structure of 1D Na_6 cluster chain with unusual short na-na distance: organic like aromaticity in inorganic metal cluster. Chem. Commun. 135–137
8. Kappes MM, Radi P, Schar M, Schumacher E (1985) Probes for electronic and geometrical shell structure effects in alkali-metal clusters. Photoionization measurements on KxLi, KxMg and KxZn (x<25). Chem Phys Lett 119:11–16
9. Khatua S, Roy DR, Bultinck P, Bhattacharjee M, Chattaraj PK (2008) Aromaticity in cyclic alkali clusters. Phys Chem Chem Phys 10:2461–2474
10. Roy DR, Shah EV, Mondal Roy S (2018) Optical activity of copoprhyrin in the light of IR and raman spectroscopy: a critical DFT investigation. Spectroch. Acta A 190:121–128
11. Watanabe HI, Inoshita T (1986) Superatom: a novel concept in materials science. Optoelectron Dev 1:33–39
12. Tung NT, Janssens E, Lievens P (2014) Dopant dependent stability of Co n TM+ (TM = Ti, V, Cr, and Mn) clusters. Appl Phys B 114(4):497–502
13. Asaduzzaman AM, Blackman JA (2010) Magnetism in binary and encapsulated Co-Mn clusters. Phys Rev B 82:134417
14. Honkala K (2014) Tailoring oxide properties: an impact on adsorption characteristics of molecules and metals. Surf Sci Rep 69(4):366
15. Henrich VE, Cox PA (1996) The Surface Science of Metal Oxides, vol 1. Cambridge University Press, Cambridge, UK
16. Danish MSS, Bhattacharya A, Stepanova D, Mikhaylov A, Grilli ML, Khosravy M, Senjyu T (2020) A systematic review of metal oxide applications for energy and environmental sustainability. Metals 10:2075–4701
17. Biswas S, Sharma P, Awasthi V, Sengar BS, Das AK, Mukherjee S (2016) Photosensitive ZnO-graphene quantum dot hybrid nanocomposite for optoelectronic applications. ChemistrySelect 1:1503–1509
18. Mohiuddin M, Kumar B, Haque H (2017) Biopolymer composites in photovoltaics and photodetectors. In: Sadasivuni KK, Ponnamma D, Kim J, Cabibihan J-J, AlMaadeed MA (eds) Biopolymer composites in electronics. Elsevier, pp 459–486
19. Tiginyanu IM, Lupan O, Ursaki VV, Chow L, Enachi M (2011) Nanostructures of Metal Oxides. In: Bhattacharya P, Fornari R, Kamimura H (eds) Comprehensive semiconductor science and Technology. Elsevier, pp 396–479
20. Stehr JE, Chen WM, Reddy NK, Tu CW, Buyanova IA (2015) Efficient nitrogen incorporation in ZnO nanowires. Sci Rep 5:13406
21. Soci C, Zhang A, Xiang B, Dayeh SA, Aplin DPR, Park J, Bao XY, Lo YH, Wang D (2007) ZnO nanowire UV photodetectors with high internal gain. Nano Lett 7:1003–1009
22. Rackauskas S, Barbero N, Barolo C, Viscardi G (2017) ZnO nanowires for dye sensitized solar cells. In nanowires-new insights. IntechOpen. https://doi.org/10.5772/67616
23. Znajdek K, Sibi'nski M, Lisik Z, Apostoluk A, Zhu Y, Masenelli B, Sedzicki P (2017) Zinc oxide nanoparticles for improvement of thin film photovoltaic structures' efficiency through down shifting conversion. Opto-Electron. Rev. 25:99–102
24. Zhang XM, Lu MY, Zhang Y, Chen LJ, Wang ZL (2009) Fabrication of a high- brightness blue-light-emitting diode using a ZnO-nanowire array grown on p-GaN thin film. Adv Mater 21:2767–2770
25. Zhang Y, Nayak TR, Hong H, Cai W (2013) Biomedical applications of Zinc oxide nanomaterials. Curr Mol Med 13:1633–1645
26. Jena P, Sun O (2020) Super atomic clusters: design rules and potential for building blocks of materials. Chem Rev 120:9021–9163
27. Li H, Li L, Pedersen A, Gao Y, Khetrapal N, Jónsson J, Zeng XC (2015) Magic- number gold nanoclusters with diameters from 1 to 3.5 nm: relative stability and catalytic activity for CO oxidation. Nano Lett. 15:682–688
28. McKee ML, Samokhvalov A (2017) Density functional study of neutral and charged silver clusters Agn with n=2–22 evolution of properties and structure. J. Phys Chem A 121:5018–5028
29. Kukreja LM, Rohlfing A, Misra P, Hillenkamp F, Dreisewerd K (2004) Cluster formation in UV laser ablation plumes of ZnSe and ZnO studied by time-of-flight mass spectrometry. Appl Phys A 78:641–644
30. Dmytruk A, Dmitruk I, Blonskyy I, Belosludov R, Kawazoe Y, Kasuya A (2009) ZnO clusters: laser ablation production and time-of-flight mass spectroscopic study. Microelectron J 40:218–220
31. Chen M, Straatsma TP, Fang Z, Dixon DA (2016) Structural and electronic property study of $(ZnO)_n$, $n \leq 168$: transition from

zinc oxide molecular clusters to ultrasmall nanoparticles. J Phys Chem C 120:20400–20418
32. Gaikwad PV, Pujari PK, Chakroborty S, Kshirsagar A (2017) Cluster assembly route to a novel octagonal two-dimensional ZnO monolayer. J Phys Cond Matter 29:335501
33. Hohenberg P, Kohn W (1964) Inhomogeneous electron gas. Phys Rev B 136:B864–B871
34. Kohn W, Sham LJ (1965) Self-consistent equations including exchange and correlation effects. Phys Rev A 140:A1133–A1138
35. Parr RG, Yang W (1989) Density functional theory of atoms and molecules. Oxford University Press, New York
36. Becke AD (1993) Density-functional thermochemistry. III. The role of exact exchange. J Chem Phys 98:5648–5652
37. Dunning Jr TH, Hay PJ (1976) in 'Modern Theoretical Chemistry', H.F. Schaefer III (Ed.), Vol. 3, Plenum, New York
38. Hay PJ, Wadt WR (1985) Ab initio effective core potentials for molecular calculations. potentials for the transition metal atoms Sc to Hg. J Chem Phys 82:270–283
39. Hay PJ, Wadt WR (1985) Ab initio effective core potentials for molecular calculations - potentials for the transition-metal atoms Sc to Hg. J Chem Phys 82:270–283
40. Frisch MJ et al (2009) Gaussian 09, Revision E.01. Gaussian Inc., Wallingford CT
41. Roy DR. Chattaraj PK (2021)'Conceptual DFT and aromaticity' in aromaticity (1st Ed.), Israel Fernández (Ed.), Elsevier: MA.
42. Pearson RG (1973) Hard and soft acids and bases. Dowden, Hutchinson and Ross, Stroutsberg, PA
43. Parr RG, Pearson RG (1983) Absolute hardness: companion parameter to absolute electronegativity. J Am Chem Soc 105:7512–7516
44. Parr RG, Szentpaly LV, Liu S (1999) Electrophilicity index. J Am Chem Soc 121:1922–1924
45. Chattaraj PK, Roy DR (2007) Update 1 of: electrophilicity index. Chem. Rev. 107:PR46–PR74
46. Chattaraj PK, Sarkar U, Roy DR, Elango M, Parthasarathi R, Subramanian V (2006) Is electrophilicity a kinetic or A thermodynamic concept? Ind J Chem A 45A:1099–1112
47. Marques MAL, Gross EKU (2004) Time-dependent density functional theory. Ann Rev Phys Chem 55:427–455
48. Casida ME, Huix-Rotllant M (2012) Progress in time-dependent density-functional theory. Annu Rev Phys Chem 63:287–323
49. Fogarasi G, Pulay P (1985) In Vibrational Spectra and Structure. Durig JR (Ed.), Elsevier: New York, Vol 13.
50. Califano S (1976) Vibrational states. Wiley, New York
51. Swinehart DF (1962) The beer-lambert law. J Chem Educ 39:333
52. Swinehart, D.F. Analytical chemistry: an introduction (Saunders Golden Sunburst Series) Skoog. In: D.A., West, D.M. & Holler, F.J. (Ed) (1999).
53. Mulliken RS (1955) Electronic population analysis on LCAO-MO molecular wave functions. I J Chem Phys 23:1833–1840